Nigerian Research Journal of Engineering and Environmental Sciences 4(1) 2019 pp. 479-486

Nigerian Research Journal of Engineering and Environmental Sciences
Journal homepage: www.rjees.com

Original Research Article

Application of Response Surface Methodology in the Optimization of Thermal Diffusivity of Low Carbon Steel Weldment during Gas Tungsten Arc Welding

***[1]Ajato, V., [1]Achebo, J.I. and [2]Obahiagbon, K.O.**
[1]Department of Production Engineering, Faculty of Engineering, University of Benin, Benin City, Nigeria
[2]Department of Chemical Engineering, Faculty of Engineering, University of Benin, Benin City, Nigeria
*ajatoforreal@gmail.com

ARTICLE INFORMATION

Article history:
Received 12 May, 2019
Revised 29 May, 2019
Accepted 10 June, 2019
Available online 30 June, 2019

Keywords:
ANOVA
Central composite design
Thermal diffusivity
Optimization
Welding

ABSTRACT

The characteristics of thermal properties of materials during welding is important, thus the need to optimize them. One of such thermal properties investigated in this study is thermal diffusivity. The thermal diffusivity of low carbon steel weldment was optimized using statistically designed experiments under the following conditions: current (150-180 A), voltage (20-23 V), and gas flowrate (10-13 L/min). A second order statistical model was developed and validated to predict the thermal diffusivity while response surface methodology (RSM) was utilized for optimizing same. Analysis of variance (ANOVA) results showed that the model was statistically significant ($p<0.05$), did not show lack of fit and was able to predict thermal diffusivity with a high level of accuracy ($R^2=0.9546$). Thermal diffusivity was significantly influenced by all three factors ($p<0.05$); although current had overall antagonistic effect while voltage and gas flowrate had a positive effect. Optimization results revealed that the optimum thermal diffusivity was 1.61×10^{-5} (m^2/s) while the optimum current, voltage and gas flowrate were 150.27 A, 23 V and 10 L/min respectively. Validation of the model indicated no significant difference between experimental observations and model prediction.

1. INTRODUCTION

It is usually desirable to produce weldments that are fit for purpose and meet specified design and usage requirements (Li et al., 2015). This makes it necessary to pay attention to the conditions of the welding process.

The welding process is a heat intensive process and is usually accompanied by various thermal characteristics, one of which is thermal diffusivity (Monika et al., 2013). Thermal diffusivity characterizes a material's ability to respond to changes in its thermal environment and this affects cooling rate, mechanical

properties, heat affected zone and heat input (Sheindlin et al., 1998). Furthermore, the welding process is usually characterised by non-uniform heat flow. The nature of heat distribution has some effect on weld morphology, weld bead geometry, cooling rate. Thus, it is desirable to control non-uniform distribution of the heat flux in order to have a quality weld (Sun et al., 2008; Suresh et al., 2012).

The thermal diffusivity of a weldment during gas tungsten arc welding (GTAW) has been reported to be affected by factors such as current, voltage, gas flow rate, welding speed, heat input etc (Trivedi and Bhabhor, 2012). It is thus necessary to optimise these factors in order to achieve optimum process conditions during welding.

The main motivation for optimizing diffusivity is to provide suitable heat flow conditions during welding in order to produce weldment of high quality. Most welders in developing nations such as Nigeria engage in welding without appropriate heat flow that will develop sound weld morphology and bead geometry required to produce quality weld (Nweze et al., 2019). The selection and setting of welding input process variables is important in order to achieve the optimal properties of weldment with good mechanical properties and conformance to requirements. Thermal diffusivity strongly affects phase transformation, cooling rate, microstructure and properties of the welds, which in turn influence the amount of distortion and residual stress created (Sheindlin et al., 1998; Trivedi and Bhabhor, 2012). In order to control the amount of weld distortion and residual stress, the weld process parameters which includes the current, voltage and gas flow rate should be appropriately selected. This is because these process parameters dominantly determine the amount of heat flow produced during welding (Sun et al., 2008).

The optimization of these welding conditions can be achieved by deploying an expert system like design of experiment coupled with response surface methodology (RSM). RSM is based on statistically designed experiments and has been found to be very useful in optimizing multivariable processes. It is employed for multiple regression analysis of quantitative data obtained from statistically designed experiments (Montgomery, 2005). RSM has been successfully applied to the optimization of many welding processes (Gunaraj and Murugan 1999; Lakshminarayanan and Balasubramanian, 2009; Dongcheol et al., 2010; Sharma and Yadava, 2013; Pujari and Patil, 2014; Achebo and Salisu, 2015; Ozigagun and Achebo, 2017).

Hence, the aim of this study was to optimize the effect of current, voltage and gas flow rate on thermal diffusivity of low carbon steel weldments during gas tungsten arc welding. A three variable central composite design coupled with response surface methodology was adopted for this purpose.

2. MATERIALS AND METHODS

2.1. Materials

The major material used in this study was a low carbon steel pipe (ASTM A106 GR SMLS) of thickness 6.35 mm. The other materials and equipment used include non-consumed tungsten electrode, shielding gas, welding machine, infra-red thermometer, thermocouple etc.

2.2. Welding Procedure

The experiment was conducted in Aveon Offshore Fabrication Yard, Rumuolumeni-Port Harcourt in Rivers State, Nigeria. The welding operations were carried out using samples of 400 mm length of 8” diameter pipe of low carbon steel with 6.35 mm thickness which were cut to size by hacksaw. The edge preparation was carried out by chamfering to a bevel angle of 30^o on each edge of the pipe in order to get a 60^o groove angle to form a single V groove type with a root face of 2.5 mm. The welding process used was gas tungsten arc welding due to its high quality, flexibility and excellent visual appearance with a minimal cleaning. Pure argon was selected as shielding gas because it is common, cheap and enhances arc stability. To ensure sound

weld, a very strong weld, the joints were properly cleaned with a grinding machine to soundness. During fit-up of the pipe, 3.2 mm core wire of electrode was used to prepare the weld joint root gap before the tack-welding of the pipe. The filler material was selected with caution to prevent excessive porosity.

2.3. Measurement Procedure

The K type thermocouples were used for measuring welding heat flow temperature. Each thermocouple was connected from the weld specimen to the digital meter for recording of temperature at same time interval. Three blind holes (each hole was 5 mm deep) were produced to the opposite of weld surface in each pipe, for the positioning of thermocouples during welding. First hole was made at 25 mm from the groove face of the prepared weld joint before weld and next holes were 1 mm apart from its previous hole in perpendicular direction to the weld joint groove axis. A total of three different layers of bead were achieved per run; root pass, hot pass and finish passes. For each run, root, hot and cap passes were used and the thermal diffusivity was measured and the average value recorded. The chosen welding process variables in this study were welding voltage, arc current and gas flow rate and their levels were set according to the experimental design.

2.4. Experimental Design

A three variable central composite design for response surface methodology was used to develop a statistical model for predicting and optimising thermal diffusivity. The range of the variables that were optimised is shown in Table 1. The experimental design made up of 20 runs was developed using Design Expert® 11.0.0 (Stat-ease, Inc. Minneapolis, USA). The coded and actual values of the independent variables were calculated using Equation 1.

$$x_i = \frac{X_i - X_o}{\Delta X} \tag{1}$$

where x_i and X_i are the coded and actual values of the independent variable respectively. X_o is the actual value of the independent variable at the centre point and ΔX_i is the step change in the actual value of the independent variable. The following generalised second order polynomial equation was used to estimate the response of the dependent variable.

$$Y_i = b_o + \sum b_i X_j + \sum b_{ij} X_i X_j + \sum b_{ii} X_i^2 + e_i \tag{2}$$

where Y_i is the dependent variable or predicted response, X_i and X_j are the independent variables, b_o is offset term, b_i and b_{ij} are the single and interaction effect coefficients and e_i is the error term.

The model parameters were estimated by applying multiple linear regression while analysis of variance (ANOVA) was used to assess the fit of the model.

Table 1: Coded and actual values of independent variables for predicting thermal diffusivity

Variables	Symbols	Coded and actual levels				
		-1.682	-1	0	+1	+1.682
Current (A)	X_1	139.77	150	165.00	180	190.23
Voltage (V)	X_2	18.98	20	21.50	23	24.02
Gas flow rate (L/min)	X_3	8.98	10	11.50	13	14.02

3. RESULTS AND DISCUSSION

3.1. Statistical Results

The results of the 20 experimental runs are shown in Table 2. Equation 3 is the second order statistical model obtained after applying multiple regression analysis to the experimental data. The equation represents thermal diffusivity as a function of current (X_1), voltage (X_2) and gas flow rate (X_3). The values of thermal diffusivity predicted by the model are also presented in Table 2 for comparison.

$$\begin{aligned} \textit{Thermal diffusivity} = {} & 2.32 - 0.021X_1 + 0.11X_2 - 0.034X_3 - 0.000095X_1X_2 \\ & - 0.00032X_1X_3 + 0.0059X_2X_3 + 0.000074X_1^2 - 0.0037X_2^2 - 0.0015X_3^2 \end{aligned} \quad (3)$$

Table 2: Experimental and predicted results for three factor CCD

Run	Factors						Response	
	Coded values			Actual values			Thermal diffusivity (m^2/s)	
	X_1	X_2	X_3	X_1	X_2	X_3	Experiment	Predicted
1	1	1	-1	180.0	23.00	10.00	1.57×10^{-5}	1.56×10^{-5}
2	1	-1	1	180.0	20.00	13.00	1.56×10^{-5}	1.55×10^{-5}
3	-1	-1	1	150.0	20.00	13.00	1.61×10^{-5}	1.62×10^{-5}
4	-1	1	1	150.0	23.00	13.00	1.67×10^{-5}	1.66×10^{-5}
5	1	-1	-1	180.0	20.00	10.00	1.57×10^{-5}	1.57×10^{-5}
6	0	0	0	165.0	21.50	11.50	1.59×10^{-5}	1.59×10^{-5}
7	0	0	-1.68	165.0	21.50	8.98	1.56×10^{-5}	1.57×10^{-5}
8	1	1	1	180.0	23.00	13.00	1.59×10^{-5}	1.59×10^{-5}
9	0	0	0	165.0	21.50	11.50	1.59×10^{-5}	1.59×10^{-5}
10	0	0	0	165.0	21.50	11.50	1.59×10^{-5}	1.59×10^{-5}
11	0	0	0	165.0	21.50	11.50	1.59×10^{-5}	1.59×10^{-5}
12	1.68	0	0	190.2	21.50	11.50	1.58×10^{-5}	1.59×10^{-5}
13	-1.68	0	0	139.7	21.50	11.50	1.69×10^{-5}	1.69×10^{-5}
14	0	0	0	165.0	21.50	11.50	1.59×10^{-5}	1.59×10^{-5}
15	0	-1.68	0	165.0	18.98	11.50	1.55×10^{-5}	1.55×10^{-5}
16	0	0	0	165.0	21.50	11.50	1.60×10^{-5}	1.59×10^{-5}
17	0	1.68	0	165.0	24.02	11.50	1.58×10^{-5}	1.58×10^{-5}
18	-1	-1	-1	150.0	20.00	10.00	1.61×10^{-5}	1.61×10^{-5}
19	-1	1	-1	150.0	23.00	10.00	1.60×10^{-5}	1.61×10^{-5}
20	0	0	1.68	165.0	21.50	14.02	1.59×10^{-5}	1.60×10^{-5}

The results obtained after performing ANOVA are presented in Table 3. Values of ''Prob. > f'' less than 0.05 indicate the model terms are significant. Values greater than 0.10 indicate the model terms are not significant. A model F-value of 23.35 and a very low probability value ($p<0.0001$) imply significant model fit. From the regression model of thermal diffusivity, the model terms X_1, X_2, X_3, X_4, and X_4^2 were significant. The interaction term X_2X_3, and quadratic terms X_1^2 and X_2^2 were also significant. The p-value of 0.0520 implies that the lack of fit was not significant. The Cor total means the total sum of squares corrected for the mean. The sum of squares is the sum of the squared deviations of each point from the mean. Hence the Cor total indicates the totals of all information corrected for the mean.

Table 4 shows that the coefficient of determination (R^2) of the model was 0.9546 indicating that the model adequately represented the relationship between the independent variables and the chosen response. An R^2 value of 0.9546 shows that the model was able to account for 95.46% of the variability observed in the response and the remaining 4.54% was as a result of chance. The coefficient of variation (C.V.) was obtained as 0.6194. This parameter indicates the degree of precision with which the experimental runs were carried out. Montgomery (2005) reported that a low value of C.V indicates a high reliability of the experiment. The Adequate precision value was obtained as 19.3659. According to Cao et al. (2009), this parameter measures the signal to- noise ratio, and a ratio greater than 4 is generally desirable.

Table 3: ANOVA results for model representing thermal diffusivity

Sources	Sum of squares	Degree of freedom	Mean squares	F value	p value
Model	0.02050	9	0.0023	23.35	0.0000
X_1	0.01056	1	0.0106	108.24	0.0000
X_2	0.00119	1	0.0012	12.17	0.0058
X_3	0.00116	1	0.0012	11.90	0.0062
X_1X_2	0.00004	1	0.0000	0.37	0.5561
X_1X_3	0.00041	1	0.0004	4.25	0.0661
X_2X_3	0.00140	1	0.0014	14.35	0.0036
X_1^2	0.00405	1	0.0040	41.48	0.0001
X_2^2	0.00100	1	0.0010	10.29	0.0094
X_3^2	0.00016	1	0.0002	1.60	0.2345
Residual	0.00098	10	0.0001		
Lack of Fit	0.00089	5	0.0002	10.09	0.0520
Pure Error	0.00009	5	0.0000		
Cor Total	0.02147	19			

Table 4: Statistical information for ANOVA for thermal diffusivity model

Parameter	Value
R-Squared	0.9546
Adjusted R-Squared	0.9137
Predicted R-Squared	0.6616
Mean	1.5900
Standard Deviation	0.0099
C.V %	0.6194
Adeq. Precision	19.3659

The adequacy of the quadratic model representing was further verified by running diagnostics on the model. The normal probability plot for the model representing thermal diffusivity is presented in Figure 1. The normal probability plot indicates whether the residuals follow a normal distribution, i.e. follow the straight line. The clustering of the points around the straight line as shown in Figure 1 shows that the residuals indeed follow a normal distribution.

Furthermore, Figure 2 shows the parity plot of the response for thermal diffusivity. It is a plot of the predicted response values versus the experimental response values. The purpose is to detect a value, or group of values, that are not easily predicted by the model. Comparison of the experimental values of the response and those predicted by the statistical model showed that there was an acceptable level of fit between the experimental

and model predicted results. This is evident from the fact that the data points all clustered around the 45° diagonal line showing that there was minimal deviation between experimental and predicted values thus indicating optimal fit of the model.

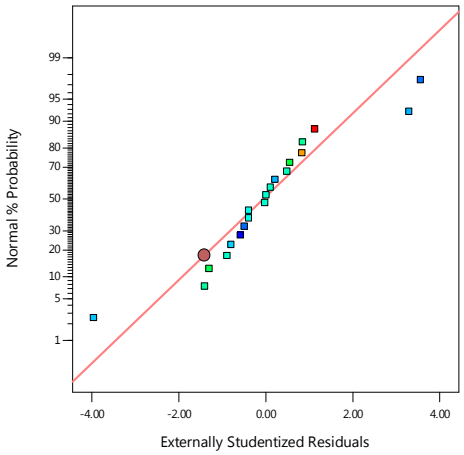

Figure 1: Normal probability plot for thermal diffusivity model

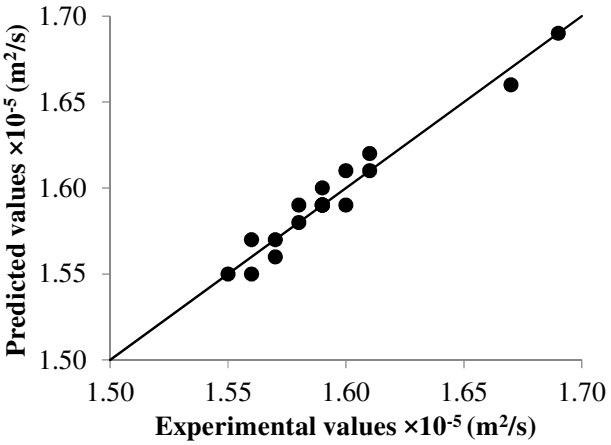

Figure 2: Parity plot for thermal diffusivity model

3.2. Effect of Independent Variables on Thermal Diffusivity

To determine the effect of the input variables on the responses, response surface plots were generated according to Equation 3. The three-dimensional (3D) plots were generated by varying two variables within the experimental range and maintaining the other one at its center point value. The resulting response surfaces showed the effect of current, gas flow rate and voltage on thermal diffusivity.

The effect of current and gas flow rate on thermal diffusivity is shown in Figure 3. The trend observed showed that an increase in current yielded a decrease in thermal diffusivity while increase in gas flow rate increased the thermal diffusivity.

The effect of gas flow rate and voltage on thermal diffusivity is shown in Figure 4. The trend observed showed that an increase in current increases the thermal diffusivity while increase in voltage increases the thermal diffusivity and vice versa.

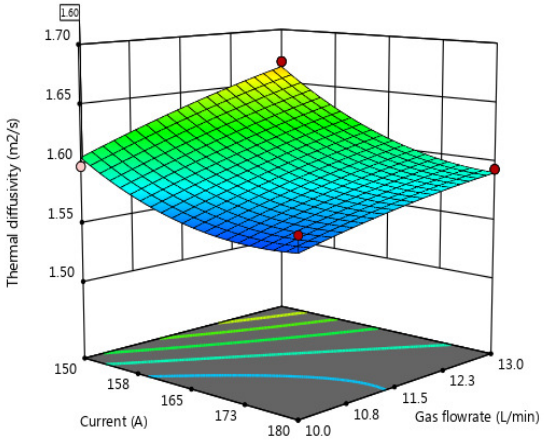

Figure 3: Effects of current and gas flow rate on thermal diffusivity

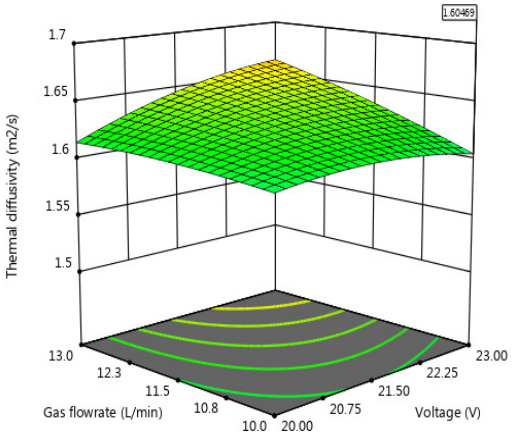

Figure 4: Effect of voltage and gas flow rate on thermal diffusivity

3.3. Optimization of Thermal Diffusivity

Numerical optimization of the response was carried out to optimize the thermal diffusivity. The values of the independent variables during numerical optimization were fixed within the experimental range. After evaluating the model graphs and the solutions suggested by the numerical optimization package, the optimum conditions were chosen as the one with the highest desirability value. The optimization results revealed that the optimum thermal diffusivity was obtained as 1.61×10^{-5} (m^2/s). This value was obtained at optimum conditions of current (150.27 A), voltage (23 V) and gas flow rate (10 L/min).

4. CONCLUSION

The modelling and optimization of the thermal diffusivity of low carbon steel during GTAW welding was carried out in this work using a three variable central composite design for response surface methodology. The second order statistical model developed was statistically significant and did not show lack of fit.

Thermal diffusivity was significantly influenced by welding current, voltage and gas flowrate. Optimum thermal diffusivity value of 1.61×10^{-5} m^2/s was obtained at optimum conditions of current (150.27 A), voltage (23 V) and gas flow rate (10 L/min). Validation of the model indicated no significant difference between experimental observations and model prediction.

5. CONFLICT OF INTEREST

There is no conflict of interest associated with this work.

REFERENCES

Achebo, J.I. and Salisu, S. (2015) Reduction of Undercuts in Fillet Welded Joints Using Taguchi Optimization Method. *Journal of Minerals and Materials Characterization and Engineering*, 3, pp. 171-179

Cao, G., Ren, N., Wang, A., Lee, D.J., Guo, W., Liu, B., Feng, Y. and Zhao, Q. (2009). Acid hydrolysis of corn stover for biohydrogen production using *Thermoanaerobacterium thermosaccharolyticum* W16. *International Journal of Hydrogen Energy*, 34, pp. 7182–7188.

Dongcheol, K., Sehun, R. and Hyunsung, P. (2010). Modeling and optimization of a GMA welding process by genetic algorithm and response surface methodology, *International Journal of Production Research*, 40(7), pp. 1699-1711.

Gunaraj, V. and Murugan, N. (1999). Prediction and comparison of the area of the heat-affected zone for the bead-onplates and bead-on-joint in submerged arc welding of pipes. *Journal of Materials Processing Technology*, 95, pp. 246-261.

Lakshminarayanan, A.K. and Balasubramanian, V. (2009). Comparison of RSM with ANN in predicting tensile strength of FSW of AA7039. *Transactions of Nonferrous metals Society of China*, 19, pp. 9-18

Li, S., Kang, Y., Zhu, G. and Kuang, S. (2015). Microstructure and Fatigue Crack Growth Behavior in Tungsten Inert Gas Welded DP780 Dual-Phase Steel. *Materials & Design*, 85, pp. 180-189.

Monika, K., Bala, C.M., Nanda, K.P. and Prahalada, R.P. (2013). The Effect of Heat input on the Mechanical Properties of MIG Welded Dissimilar Joints. *International Journal of Engineering Research & Technology,* 2, pp. 1406-1413

Montgomery, D.C. (2005). Design and Analysis of experiments, 6th ed., New York: John Wiley & Sons, Inc.

Nweze, S., Achebo J.I. and Obahiagbon, K.O. (2019). Application of response surface methodology in the optimization and prediction of percentage (%) weld dilution of TIG mild steel weldments. *International Journal of Scientific & Engineering Research*, 10(1), p. 312

Ozigagun, A. and Achebo, J.I. (2017). Optimization of weld bead undercuts in tungsten inert gas mild steel weld using response surface methodology. *Nigerian Research Journal of Engineering and Environmental Sciences*, 2(2), pp. 571-577.

Pujari, K.S. and Patil, D.V. (2014). Effect of GTAW Process Parameters on Weld Bead Geometry of AA 7075-T6 Weldments. *International Journal of Engineering Research & Technology*, 3(8), pp. 1097-1109

Sharma, A. and Yadava, V. (2013). Modelling and optimization of cut quality during pulsed Nd:YAG laser cutting of thin Al-alloy sheet for curved profile. *Optics and Lasers in Engineering*, 51, pp. 77–88.

Sheindlin, M., Halton, D., Musella, M. and Ronchi, C. (1998) Advances in the use of Laser-Flash Techniques for Thermal Diffusivity Measurement. *Review of Scientific Instruments*, 69, pp. 1426-1436

Sun, H., Song, G. and Zhang, L.F. (2008). Effects of Oxide Activating Flux on Laser Welding of Magnesium Alloy. *Science and Technology of Welding and Joining*, 13, pp. 305-311

Suresh K., L., Verma, S M., Suryanarayana, B. and Kiran Kumar, B. (2012). Analysis of Welding Characteristics on Stainless Steel for the Process of TIG and MIG with Dye Penetrate Testing. *International Journal of Engineering and Innovative Technology*, 2, pp. 283-290.

Trivedi, P. T. and Bhabhor, A. P. (2012). Experimental Investigation of Process Parameters on Weld Bead Geometry for Aluminium Using GTAW. *Journal of Science and Research*, 3(5), pp. 803-809.